arXiv:0909.3176v3 [gr-qc] 9 Mar 2010

Local free-fall temperature of a RN-AdS black hole

Yong-Wan Kim*[1], Jaedong Choi†[2] and Young-Jai Park‡[3],

[1]Institute of Basic Science and School of Computer Aided Science,
Inje University, Gimhae 621-749, Korea,
[2]Center of Defense Management, Korea Institute for Defense Analysis,
39 Hoegiro Dongdaemun Seoul 130-010, Korea,
and
[3]Department of Physics and BK21 Program Division,
Sogang University, Seoul 121-742, Korea,
Service Systems Management and Engineering and WCU Program Division,
Graduate School of Business, Sogang University, Seoul 121-742, Korea

March 10, 2010

ABSTRACT

We use the global embedding Minkowski space (GEMS) geometries of a (3+1)-dimensional curved Reissner-Nordström(RN)-AdS black hole spacetime into a (5+2)-dimensional flat spacetime to define a proper local temperature, which remains finite at the event horizon, for freely falling observers outside a static black hole. Our extended results include the known limiting cases of the RN, Schwarzschild–AdS, and Schwarzschild black holes.

PACS number(s): 04.70.Dy, 04.20.Jb, 04.62.+v
Keywords: Reissner–Nordström–AdS, Global flat embedding, Unruh effect

*Electronic address: ywkim65@gmail.com
†Electronic address: choijdong@yahoo.co.kr
‡Electronic address: yjpark@.sogang.ac.kr

1 Introduction

Unruh [1, 2] proposed that a uniformly accelerated observer with proper acceleration a in flat spacetime will detect thermal radiation at the so-called Unruh temperature, $T_U = \frac{a}{2\pi}$. After his work, it has been known that a thermal Hawking effect on a curved manifold [3] can be looked at as an Unruh effect in a higher dimensional flat space-time. Non-trivial works of isometric embeddings of the RN [4], RN-AdS [5], Kerr [6] black holes and M2-, D3-, M5-branes [7] into flat spaces have been studied to get some insight of the global aspect of the spacetime geometries. Moreover, several authors [8, 9, 10, 11] have also shown that global embedding Minkowski space (GEMS) approach [12, 13, 14, 15, 16, 17, 18, 19, 20, 21] of which a hyperboloid in a higher dimensional space corresponds to original curved space could provide a unified derivation of temperature for a wide variety of curved spaces. Still, the GEMS approach has been used to understand the relation between the thermal Hawking temperature and the Unruh Effect [22, 23, 24, 25, 26, 27, 28].

Recently, Brynjolfsson and Thorlacius have used the global embedding of Schwarzschild(-AdS), and RN black holes spacetime into higher dimensional flat spacetimes to define a local temperature for freely falling observers outside a static black hole, separately [29]. In fact, they have successfully defined a local temperature by using the fact that there are special turning points of radial geodesics where freely falling observers are momentarily at rest with respect to black hole. As a result, they have shown that the local free-fall temperature remains finite at the event horizon, while it approaches the Hawking temperature in asymptotically flat spacetime. Moreover, they have also shown that freely falling observers outside an AdS black hole do not see any high-temperature thermal radiation even if the Hawking temperature of such black holes can be arbitrarily high. Very recently, Greenwood and Stojkovic have also shown for the case of the Schwarzschild black hole that the temperature is finite at the horizon in Eddington-Finkelstein reference frame, where the observer is not accelerated [30].

On the other hand, ever since the discovery that thermodynamic properties of black holes in anti-de Sitter (AdS) spacetime are dual to those of a field theory in one dimension fewer, there has been of much interest in RN-AdS black hole [31], which now becomes a prototype example [32, 33, 34, 35, 36, 37, 38, 39, 40, 41] to study this AdS/CFT correspondence

[42].

In this paper we will use the global embedding of the RN-AdS black hole spacetime into a (5+2) dimensional flat spacetime [5] to define a desired local temperature for observers in radial free fall outside a static black hole as a generalization of the previous work [29]. As a result, this generalization includes the known limiting cases [29] of the Schwarzschild-AdS (SAdS) and RN black holes in (5+2)-dimensions, and Schwarzschild black hole in (5+1)-dimensions through the successive truncations. In Sec. 2, we briefly recapitulate the structure of the RN-AdS black holes, which are classified by the charge Q with a negative cosmological constant Λ. In Sec. 3, we first shortly review the $(3+1)$ dimensional RN-AdS embedding into the (5+2) dimensional flat space, which had been obtained by two of us [5], and use this GEMS method to define a proper local temperature for observers in free fall outside a static black hole. In Sec. 4, we also show that our results in the GEMS of the RN-AdS space systematically include those of the known limiting GEMS geometries, which are the RN, SAdS, and Schwarzschild, through the successive truncation procedure of parameters in the original curved space. Finally, we present summary in Sec. 5.

2 Structure of RN-AdS black hole

Let us consider the line element of the (3+1) dimensional RN-AdS spacetime with a negative cosmological constant $\Lambda = -3/l^2$ [31] as

$$ds_4^2 = -f(r,m,Q,l)dt^2 + f^{-1}(r,m,Q,l)dr^2 + r^2(d\theta^2 + \sin^2\theta d\phi^2), \qquad (1)$$

where $f(r,m,Q,l)$ is given by

$$f(r,m,Q,l) = 1 - \frac{2m}{r} + \frac{Q^2}{r^2} + \frac{r^2}{l^2}. \qquad (2)$$

Here, m and Q are the black hole mass and charge, respectively.

This space-time is asymptotically described by the AdS. Then, the inner (r_-) and the outer (r_+) horizons are obtained from the condition of $f(r_\pm,m,Q,l) = 0$ [43]. The Arnowitt-Deser-Misner (ADM) mass of the RN-AdS black hole and its event horizon radius $r = r_+$ are related as

$$m = \frac{1}{2}\left[r_+ + \frac{r_+^3}{l^2} + \frac{Q^2}{r_+}\right]. \qquad (3)$$

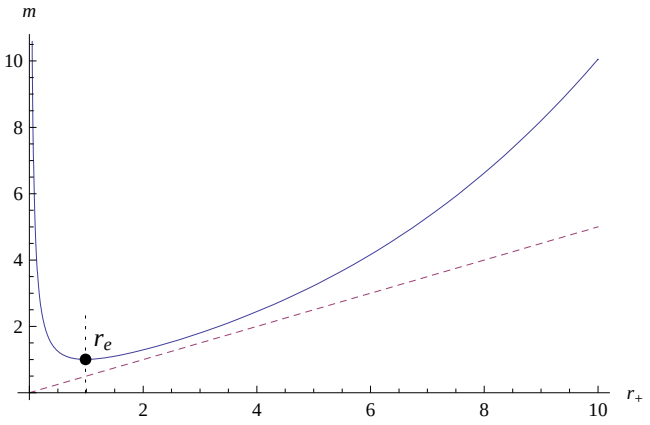

Figure 1: Mass function for the RN-AdS black hole with $Q = 1 < Q_c = l/6$ and $l = 10$. Dashed line is for the Schwarzschild black hole. The extremal radius r_e is denoted by the symbol $\bullet$.

In this work we consider the case of fixed-charge ensemble [44] with $Q < Q_c$ where Q_c will be determined in Eq. (10).

The surface gravity k_H is given by

$$k_H(r_+, Q, l) \equiv \frac{1}{2}\left.\frac{df}{dr}\right|_{r=r_+} = \frac{(r_+^2 - Q^2)l^2 + 3r_+^4}{2r_+^3 l^2}. \tag{4}$$

Then, the Hawking temperature T_H, which is the temperature of the radiation as measured by asymptotic observer, is given by

$$T_H(r_+, Q, l) = \frac{k_H}{2\pi} = \frac{1}{4\pi}\left(\frac{1}{r_+} - \frac{Q^2}{r_+^3} + \frac{3r_+}{l^2}\right). \tag{5}$$

Note that the Hawking temperature of large AdS black holes grows linearly with r_+, and becomes arbitrarily high for very large black holes. However, as we will see below, this does not mean that the physical temperature measured by an observer in free fall becomes large outside large AdS black holes [29].

On the other hand, the local fiducial temperature, which is the temperature of the radiation as measured by a fiducial observer, is given by

$$T_{FID}(r) = \frac{T_H}{\sqrt{f(r, m, Q, l)}}. \tag{6}$$

Here, the fiducial observer means an observer who remains at rest with respect to black hole at a fixed distance. Note that the fiducial temperature T_{FID} diverges at the black hole event horizon. On the other hand, in asymptotically flat spacetime T_{FID} approaches the Hawking temperature asymptotically far away from the black hole, while in asymptotically AdS spacetime T_{FID} goes to zero far away from the black hole.

Moreover, using the outer and inner horizons, the mass, charge, and Hawking temperature are expressed as follows

$$\begin{aligned} m(r_+, r_-) &= \frac{1}{2}\left[r_+ + r_- + \frac{r_+^4 - r_-^4}{l^2(r_+ - r_-)}\right], \\ Q^2(r_+, r_-) &= r_+ r_- \left[1 + \frac{r_+^3 - r_-^3}{l^2(r_+ - r_-)}\right], \\ T_H(r_+, r_-) &= \frac{r_+ - r_-}{4\pi l^2 r_+^2}\left(l^2 + 3r_+^2 + 2r_+ r_- + r_-^2\right), \end{aligned} \tag{7}$$

respectively. For the degenerate case ($r_+ = r_- = r_e$), we have an extremal black hole with $m = m_e = r_e$ as shown in Fig.1. In general, one has an inequality of $m > m_e$. Then, using the Eqs. (3) and (5), the heat capacity $C_Q = (dm/dT_H)_Q$ for the fixed-charge Q takes the form

$$C_Q(r_+, Q, l) = 2\pi r_+^2 \left[\frac{3r_+^4 + l^2(r_+^2 - Q^2)}{3r_+^4 - l^2(r_+^2 - 3Q^2)}\right]. \tag{8}$$

The global features of thermodynamic quantities for $Q < Q_c = l/6$ are shown in Fig. 2. Here we observe the local minimum $T_H = T_0$ at $r_+ = r_s$ (SAdS-like black hole), in addition to the zero temperature $T_H = 0$ at $r_+ = r_e$(extremal RN-like black hole) and the local maximum $T_H = T_D$ at $r_+ = r_D$ (Davies' point of RN black hole). Therefore, it seems to be a combination of the RN and SAdS black holes [41].

Furthermore, we observe that $C_Q = 0$ and $T_H = 0$ at $r_+ = r_e$, where

$$r_e^2 = \frac{l^2}{6}\left(-1 + \sqrt{1 + \frac{12Q^2}{l^2}}\right), \tag{9}$$

and the heat capacity blows up at $r_+ = r_D$ and r_s, where these satisfy

$$r_D^2 = \frac{l^2}{6}\left(1 - \sqrt{1 - \frac{36Q^2}{l^2}}\right), \; r_s^2 = \frac{l^2}{6}\left(1 + \sqrt{1 - \frac{36Q^2}{l^2}}\right). \tag{10}$$

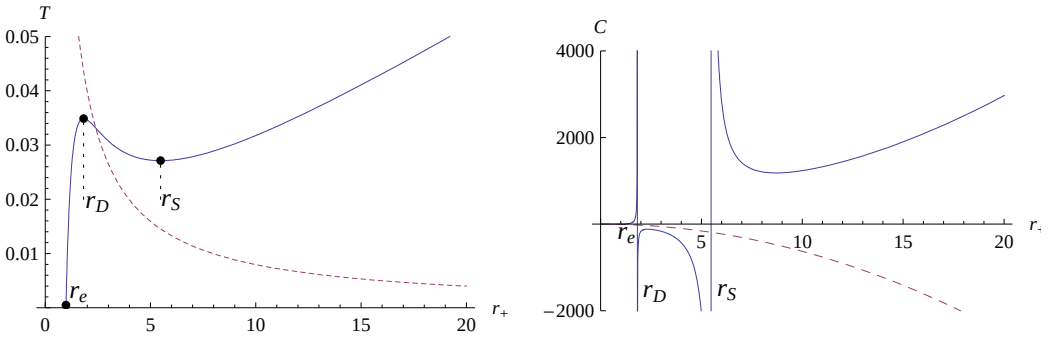

Figure 2: Thermodynamic quantities of the RN-AdS black hole as function of horizon radius r_+ with fixed $Q = 1 < Q_c$ and $l = 10$: temperature T_H with $T_D = 0.035$, $T_s = 0.027$, and heat capacity C. Dashed curves are for the Schwarzschild black holes.

These points exist only for $Q \leq Q_c = l/6$. For the $Q = Q_c$ case, we have $r_D = r_s = l/\sqrt{6}$. The local stability is usually determined by the positive sign of heat capacity by considering evaporation and absorbing processes of a black hole [45]. For example, the heat capacity of the Schwarzschild black hole is $-2\pi r_+^2$, which means that this isolated black hole is not in equilibrium in asymptotically flat spacetimes. Based on the local stability of heat capacity, the RN-AdS black holes of $Q < Q_c$ can be split into stable small AdS black hole with $C_Q > 0$ being in the region of $r_e < r_+ < r_D$, intermediate unstable black hole with $C_Q < 0$ in the region of $r_D < r_+ < r_s$, and stable large AdS black hole with $C_Q > 0$ in the region of $r_+ > r_s$.

Note that large AdS black holes with $r_+ \gg l$ [46] correspond to high-temperature thermal states in the dual gauge theory [42], while small AdS black holes with $r_+ \ll l$ can be viewed as more-or-less ordinary RN black holes in a cosmological background with a negative cosmological constant.

3 Local Temperature of RN-AdS Black Hole in the GEMS Approach

Ten years ago, through the GEMS approach, which makes the curved spacetime possibly embedded in a higher dimensional flat spacetime [12, 13, 14,

15, 16, 17], two of us had obtained a $(5+2)$-dimensional isometric embedding [5] of the RN-AdS spacetime with metric $\eta_{IJ} = \mathrm{diag.}(-1,1,1,1,1,1,-1)$ $(I,J = 0,1,...,6)$ as

$$
\begin{aligned}
z^0 &= k_H^{-1}\sqrt{f(r,m,Q,l)}\sinh(k_H t),\\
z^1 &= k_H^{-1}\sqrt{f(r,m,Q,l)}\cosh(k_H t),\\
z^2 &= \int dr \left(\frac{Q^2 l^2}{[rr_H(r^2+rr_H+r_H^2)+(rr_H-Q^2)l^2]} \right.\\
&\quad \left. + \frac{r_H^2 l^2 (r^2+rr_H+r_H^2)[(r_H^2-Q^2)^2 l^4 + r_H^6(r_H^2+2l^2)]}{r^2[3r_H^4+(r_H^2-Q^2)l^2]^2[rr_H(r^2+rr_H+r_H^2)+(rr_H-Q^2)l^2]} \right)^{1/2},\\
z^3 &= r\sin\theta\cos\phi,\\
z^4 &= r\sin\theta\sin\phi,\\
z^5 &= r\cos\theta,\\
z^6 &= \int dr \left(\frac{Q^2 l^4 r_H^6[4(rr_H-Q^2)l^2+10r^4+2rr_H(r^2+rr_H+2r_H^2)]}{r^4[3r_H^4+(r_H^2-Q^2)l^2]^2[rr_H(r^2+rr_H+r_H^2)+(rr_H-Q^2)l^2]} \right.\\
&\quad \left. + \frac{rr_H(r^2+rr_H+r_H^2)(4r_H^6 l^2+[3r_H^4+(r_H^2-Q^2)l^2]^2)}{[3r_H^4+(r_H^2-Q^2)l^2]^2[rr_H(r^2+rr_H+r_H^2)+(rr_H-Q^2)l^2]} \right)^{1/2}
\end{aligned}
\tag{11}
$$

with an additional spacelike z^2 and a timelike z^6 dimensions. Here, we have denoted the outer horizon r_+ as r_H. As a result, the (3+1)-dimensional curved spacetime of the RN-AdS is seen as the hyperboloid embedded in the (5+2)-dimensional flat spacetime. It would be easily verified inversely that the following flat metric in the (5+2)-dimensional space defined as the coordinates (11) gives the original RN-AdS metric (1) correctly

$$
ds_7^2 \equiv \eta_{IJ} dz^I dz^J = ds_4^2. \tag{12}
$$

This equivalence between the (5+2)-dimensional flat embedding spacetime and original (3+1)-dimensional curved one is well-established for the definition of isometric embedding, mathematically developed by several authors [7, 47, 48, 49].

Now, let us consider a freely falling observer dropped from rest at $\tau = 0$ and $r = r_0$. Note that this observer differs from a fiducial observer who remains at rest with respect to the black hole at a fixed distance. The

equations for the orbit are

$$\frac{dt}{d\tau} = \frac{\sqrt{f(r_0,m,Q,l)}}{f(r,m,Q,l)}, \tag{13}$$

$$\frac{dr}{d\tau} = \sqrt{f(r_0,m,Q,l)-f(r,m,Q,l)}. \tag{14}$$

Then, the 7-acceleration a_7^I definded in the $(5+2)$-dimensional embedded flat spacetime is spacelike for all timelike orbits, and at the turning point $r=r_0$, where the observer is dropped from rest, its squared magnitude $a_7^2(=\eta_{IJ}a_7^I a_7^J)$ is given by

$$\begin{aligned} a_7^2 = & \Big[4(1+x)-(c^2+1)(c^2+5)x^2-(c^2+1)^2x^3(1+x+x^2) \\ & -b^2(1+b+b^2+c^2)^2x^2(1+x+x^2+x^3+4x^5) \\ & +2b(1+b+b^2+c^2)x^2(2+4x+(c^2+1)(1+x+x^2+x^3+2x^4))\Big] \\ & /\left[4c^2r_H^2(bx-1)\left(1+(1+b)x+\left(1+b+b^2+c^2\right)x^2\right)\right], \end{aligned} \tag{15}$$

where $x\equiv r_H/r$, $Q^2\equiv bl^2(1+b+b^2+c^2)/c^4$, $b\equiv r_-/r_H$, and $c\equiv l/r_H$.

Taking the local temperature $T_{FFAR}=a_7/2\pi$ measured by the freely falling observer at rest to be the local Unruh temperature of the corresponding observer in the (5+2)-dimensional flat spacetime, we obtain

$$\begin{aligned} T_{FFAR}^2 = & \Big[4(1+x)-(c^2+1)(c^2+5)x^2-(c^2+1)^2x^3(1+x+x^2) \\ & -b^2(1+b+b^2+c^2)^2x^2(1+x+x^2+x^3+4x^5) \\ & +2b(1+b+b^2+c^2)x^2(2+4x+(c^2+1)(1+x+x^2+x^3+2x^4))\Big] \\ & /\left[16\pi^2c^2r_H^2(bx-1)\left(1+(1+b)x+\left(1+b+b^2+c^2\right)x^2\right)\right]. \end{aligned} \tag{16}$$

In the limit of $c\to\infty$ (or, $l\to\infty$), the temperature is reduced to the isometrically flat embedded one for the RN

$$T_{FFAR}^2 = \frac{(1-b)^2(1+x+x^2+x^3)-4bx^4+4b^2x^5}{16\pi^2r_+^2(1-bx)}. \tag{17}$$

In the limit of $b\to 0$ (or, $Q\to 0$), the temperature becomes the corresponding flat embedded one for the SAdS

$$T_{FFAR}^2 = \frac{-4(1+x)+(c^2+1)(c^2+5)x^2+(c^2+1)^2x^3(1+x+x^2)}{16\pi^2c^2r_H^2[1+x+(c^2+1)x^2]}. \tag{18}$$

These limits are exactly the same with the ones obtained in [29].

The free-fall temperature (16) can be further simplified in the two interesting limits: at spacial infinity $r \to \infty$ ($x \to 0$) and at event horizon $r \to r_H$ ($x \to 1$). At spacial infinity $r \to \infty$, one obtains imaginary temperature as

$$T^2_{FFAR} \to -\frac{1}{4\pi^2 l^2}, \tag{19}$$

which is allowed for a geodesic observer who follows a spacelike motion in empty AdS space [8]. Note also that from $l = c\ r_H$ as c increases T^2_{FFAR} becomes negatively small, while as c decreases T^2_{FFAR} becomes negatively large, however, not possibly positive. On the other hand, at event horizon, $r \to r_H$, one obtains

$$T^2_{FFAR} \to \frac{(1-2b)c^2 - 2b(1+b+b^2)}{4\pi^2 l^2}, \tag{20}$$

which has always imaginary temperature when $b \geq 1/2$. However, when $0 < b < 1/2$, the free fall temperature T^2_{FFAR} turns out to be real and positive if the following condition is satisfied

$$c \geq \sqrt{\frac{2b(1+b+b^2)}{1-2b}}. \tag{21}$$

Now, let us look into their general features in detail for the extended case of the RN-AdS black holes, which are described by the parameters b and c. First, Fig. 3 shows the free fall temperature T^2_{FFAR} of the RN-AdS black holes, seen by the freely falling observer from the rest, in units of the Hawking temperature T^2_H given by

$$T_H = \frac{(1-b)(3+2b+b^2+c^2)}{4\pi c^2 r_H}. \tag{22}$$

On the other hand, Fig. 4 shows the ratio of the free fall temperature T^2_{FFAR} to the Hawking temperature T^2_H from the horizon ($x = 1$) to the spacial infinity ($x = 0$) according to the different values of c. In particular, for the $b = 0.4$ case, representing one of the RN-AdS black holes, two bold curves of left panel in Fig. 3 are for $c = 100, 10$, which correspond to small black holes. On the other hand, the curves of right panel in Fig. 3 are for $c = 10, 2.5$, where the last $c = 2.5$ case is part of large black holes. The curve of $c = 1.9$

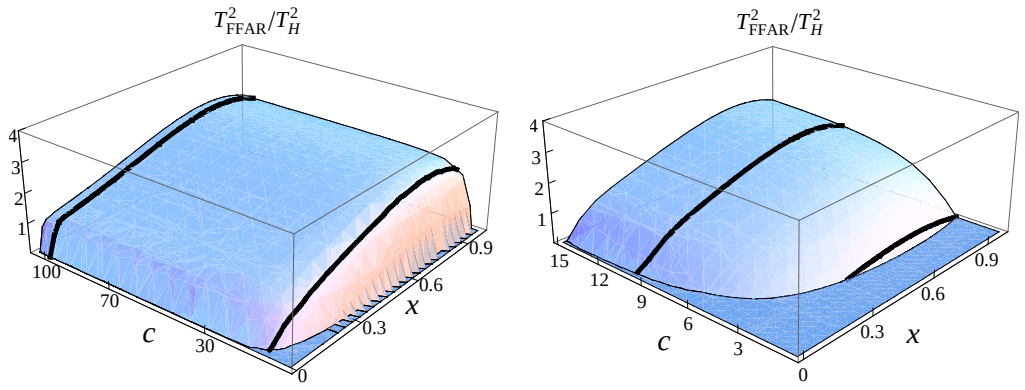

Figure 3: Free-fall temperature T^2_{FFAR} in units of T^2_H for the $b = 0.4$ case. The solid curves are for $c = 100, 10, 2.5$ describing the permitted radiation range x.

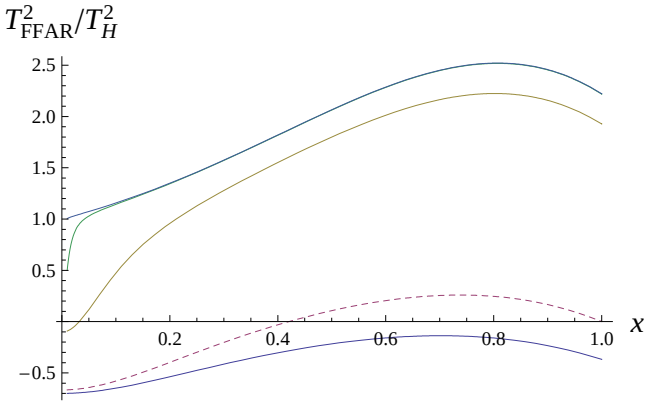

Figure 4: Slices of free-fall temperature T^2_{FFAR} for the $b = 0.4$ case. The curves are for $c = 1000, 100, 10, 2.5, 1.9$ from top to down. The curve for $c = 1000$ actually represents the Schwarzschild limit, and the dashed curve describes that the free fall temperature T^2_{FFAR} vanishes at event horizon $x = 1$.

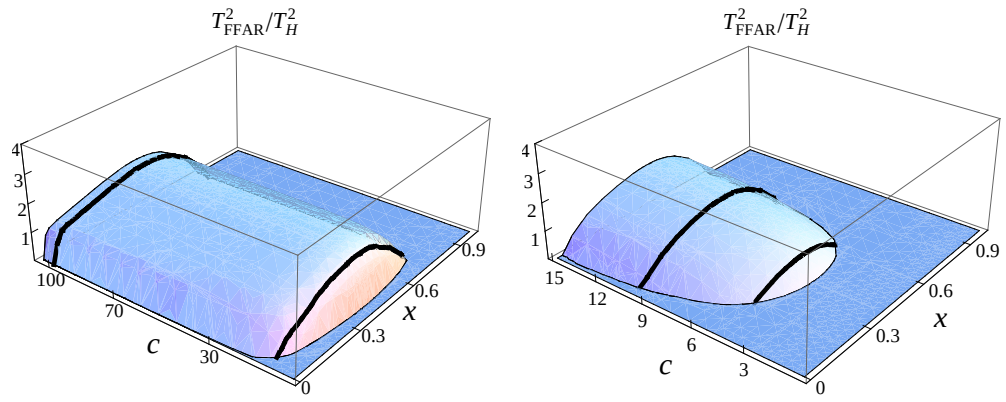

Figure 5: Free-fall temperature T^2_{FFAR} for the $b = 0.6$ case. The solid curves are for $c = 100, 10, 5$.

is not shown in Fig. 3, but shown in Fig. 4 because it is not satisfied Eq. (21) and thus has always negative for all x. This reflects the fact of no thermal radiation. In Fig. 4, the dashed curve is for $c = 2.5$ in which value the free fall temperature T^2_{FFAR} at event horizon vanishes. When $c > 2.5$, the temperatures T^2_{FFAR} are all real and finite as shown in Fig. 4 at event horizon. The curve for $c = 1000$ in Fig. 4 represents the Schwarzschild limit.

Figs. 5 and 6 describe the RN-AdS black holes for the $b = 0.6$ case. Two bold curves of left panel in Fig. 5 describe the squared free-fall temperatures for $c = 100, 10$, and the last curve of right panel is for $c = 5$. Compared with the RN-AdS case with $b = 0.4$, all these local temperatures become negative for freely falling observer before arriving at the event horizon showing that the observer feels no thermal radiation near the horizon. On the other hand, Figs. 7 and 8 show the squared free fall temperatures for the RN-AdS black holes for fixed $c = 100$, $c = 10$ cases, respectively, while for varying b. In Fig. 8, the curve of $b = 1$ has been not shown because it has very large negative value.

Furthermore, Fig. 9 specializes to the $c \to \infty$ case, the RN limit. At spacial infinity ($x \to 0$), the free fall temperature coincides with the Hawking

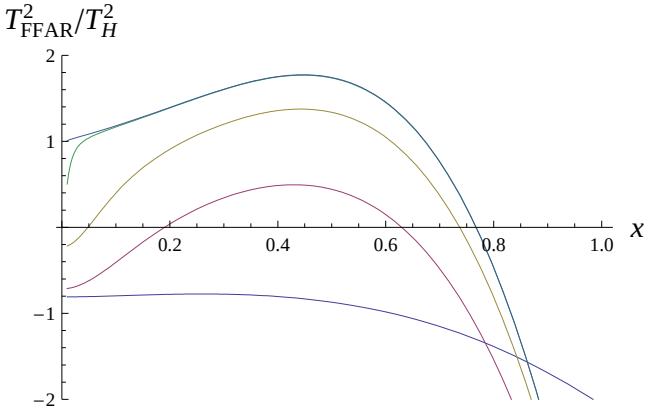

Figure 6: Slices of free-fall temperature T^2_{FFAR} for the $b = 0.6$ case. The curves are for the $c = 1000, 100, 10, 5, 1$ cases from top to down.

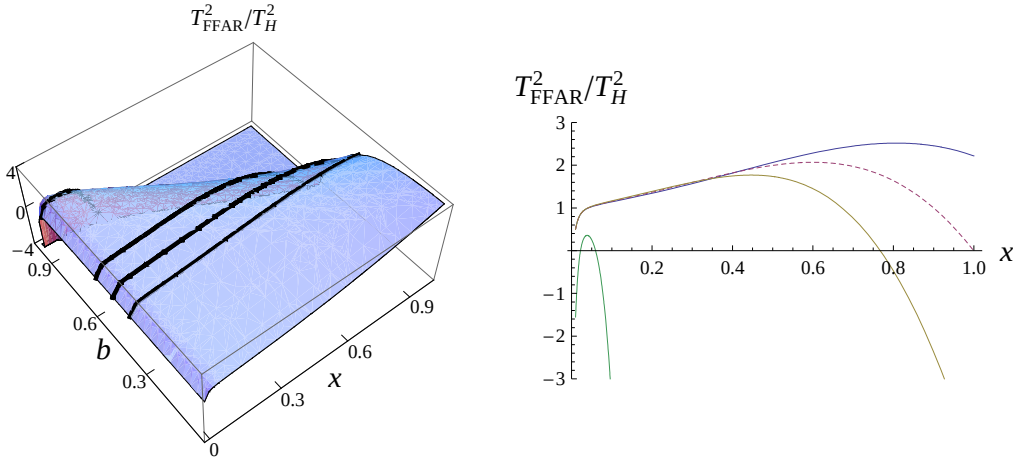

Figure 7: Left panel: Free -fall temperature T^2_{FFAR} for the RN-AdS black holes with $c = 100$. The solid curves are for the $b = 0.4, 0.5, 0.6, 1$ cases. Right panel: Cross section of free-fall temperature T^2_{FFAR} for the $b = 0.4, 0.5, 0.6, 1$ cases from top to down. The dashed curve describes T^2_{FFAR} vanishes at event horizon $x = 1$.

temperature

$$T_{FFAR} \to T_H = \frac{r_+ - r_-}{4\pi r_+^2}. \tag{23}$$

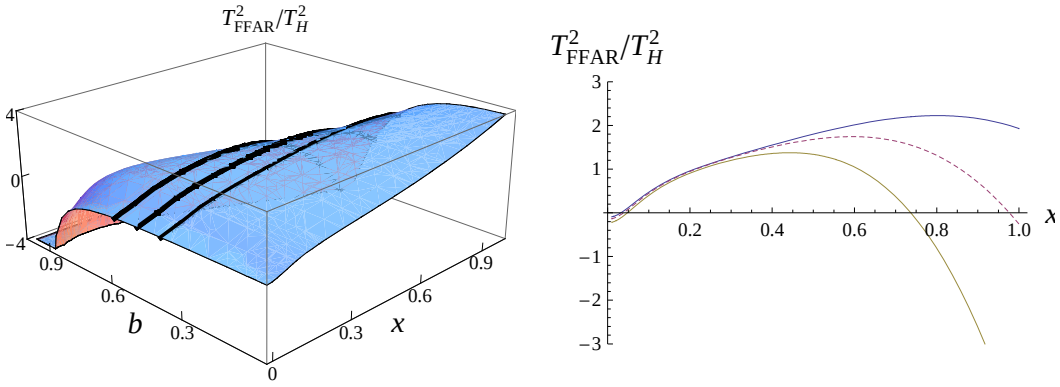

Figure 8: Left panel: Free fall temperature T^2_{FFAR} for the RN-AdS black holes with $c = 10$. The solid curves are for the $b = 0.4, 0.5, 0.6$ cases. Right panel: Cross section of free fall temperature T^2_{FFAR} for the $b = 0.4, 0.5, 0.6$ cases from top to down. The dashed curve describes T^2_{FFAR} vanishes at event horizon $x = 1$.

As a result, the difference between Fig. 7 ($c = 100$) and Fig. 9 ($c \to \infty$) lies in the behavior of temperature in the asymptotically far away from the black holes: the former T^2_{FFAR}/T^2_H goes to zero, however, the latter goes to one, which means that the free fall and Hawking temperatures coincide.

On the other hand, Figs. 10 and 11 describe the SAdS limit of $b \to 0$. Its asymptotic limit $x \to 1$ of the local free temperature gives exactly Eq. (19), while on event horizon one has

$$T^2_{FFAR} \to \frac{1}{4\pi^2 r_+^2}, \tag{24}$$

as expected. For a small AdS black hole with $r_H \ll l$ (or, large c), the horizon area reduces to that of a RN black hole in asymptotically flat spacetime with $r_H \approx m + \sqrt{m^2 - Q^2}$, and (16) reduces to

$$T_{FFAR} \to \frac{1}{2\pi r_H}\,(1-2b)^{\frac{1}{2}} \approx 2T_H \tag{25}$$

at the event horizon with $b \to 0$ ($Q^2 \ll r_H^2$). This can be seen in Fig. 11 near $x = 1$ when $c = 1.000$ (or, $c = 100$) and $b = 0$. On the other hand, for

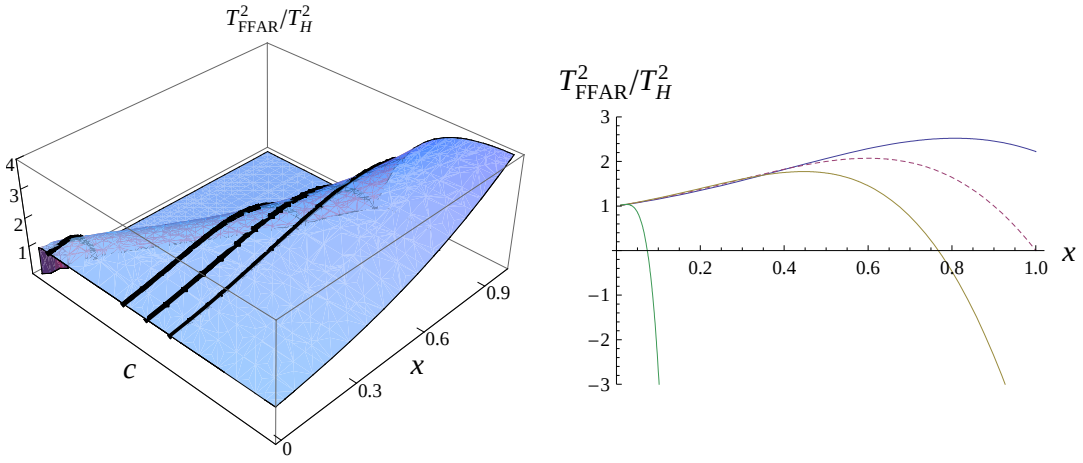

Figure 9: Left panel: Free-fall temperature T^2_{FFAR} for the RN black holes ($c \to \infty$). The solid curves are for the $b = 0.4, 0.5, 0.6, 1$ cases. Right panel: Cross section of free-fall temperatures T^2_{FFAR} for the $b = 0.4, 0.5, 0.6, 1$ cases from top to bottom.

a large AdS black hole with $r_H \gg l$ (or, small c) [46], we find that at the event horizon

$$T_{FFAR} \to \frac{1}{2\pi r_H} \ll T_H, \tag{26}$$

which makes the ratio of T^2_{FFAR}/T^2_H approximately zero.

Finally, we reobtain the Schwarzschild limit without the cosmological constant from the SAdS embedding with the $l \to \infty$ ($c \to \infty$) limit, or the RN embedding with the $Q = 0$ ($b = 0$) one. Taking the $c \to \infty$ limit in Eq. (18), or the $b = 0$ limit in Eq. (17), the T^2_{FFAR} and T_H reduce to the Schwarzschild one as follows

$$T^2_{FFAR} = \frac{1 + x + x^2 + x^3}{16\pi^2 r_H^2}, \tag{27}$$

which also coincide with the previous work [29]. As a final comment, we have checked that the embedding functions (11) have exactly the same form of the ones in Ref. [5, 29] when taking the limit referred in this work.

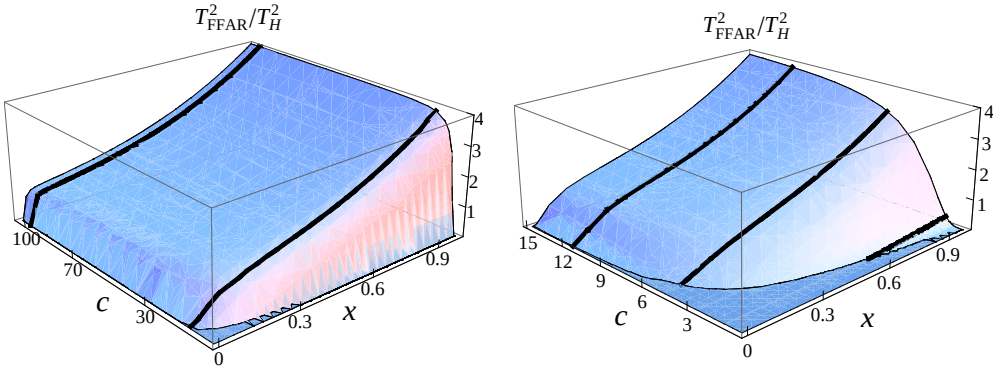

Figure 10: Free-fall temperature T^2_{FFAR} for $b = 0$ in units of T^2_H, which corresponds to the case of the SAdS black holes. The solid curves are for the $c = 100, 10, 5, 1$ cases.

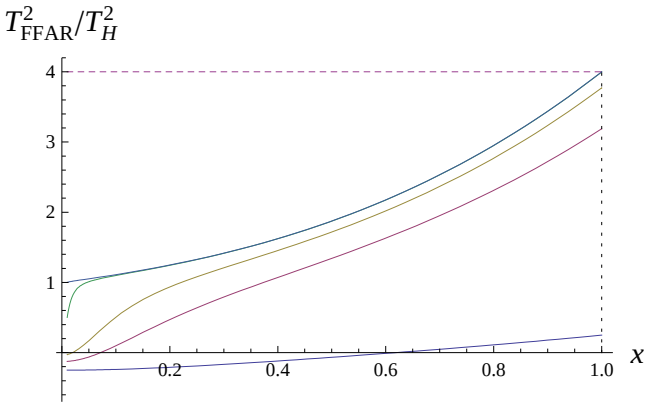

Figure 11: Slices of free-fall temperature T^2_{FFAR} for the $b = 0$ case in units of T^2_H. The curves are for the $c = 1000, 100, 10, 5, 1$ cases from top to down.

4 Summary

In summary, we have used the global embedding of the RN-AdS black hole spacetime into a (5+2) dimensional flat spacetime to define a desired local

temperature for observers in radial free fall outside a static black hole as a generalization of the previous work [29]. We have also shown that our extended results in the GEMS of the RN-AdS space systematically include those of the known limiting GEMS geometries, which are the RN, SAdS, Schwarzschild, through the successive truncation procedure of parameters in the original curved space.

Acknowledgement

The authors thank L. Thorlacius for helpful communication. Y.-W. Kim was supported by the Korea Research Foundation Grant funded by Korea Government (MOEHRD): KRF-2007-359-C00007. Y.-J. Park was supported by the Korea Science and Engineering Foundation (KOSEF) grant funded by the Korea government (MEST) (No. 20090083765 and R31-20002).

References

[1] W. G. Unruh, Phys. Rev. D **14**, 870 (1976).

[2] P. C. W. Davies, J. Phys. A **8**, 609 (1975).

[3] S. W. Hawking, Commun. Math. Phys. **43**, 199 (1974).

[4] S. Deser and O. Levin, Phys. Rev. D **59**, 0640004 (1999).

[5] Y. W. Kim, Y. J. Park and K. S. Soh, Phys. Rev. D **62** 104020 (2000).

[6] G. W. Gibbons, C. A. R. Herdeiro and C. Rebelo, Phys. Rev. D **80**, 044014 (2009).

[7] L. Andrianopoli, M. Derix, G. W. Gibbons, C. Herdeiro, A. Santambrogio, and A. Van Proeyen, Class. Quantum Grav. **17**, 1875 (2000).

[8] S. Deser and O. Levin, Class. Quantum Grav. **14**, L163 (1997).

[9] S. Deser and O. Levin, Class. Quantum Grav. **15**, L85 (1998).

[10] M. Beciu and H. Culetu, Mod. Phys. Lett. A **14**, 1 (1999).

[11] P. F. Gonzalez-Diaz, Phys. Rev. D **61**, 024019 (1999).

[12] E. Kasner, Am. J. Math. **43**, 130 (1921).

[13] C. Fronsdal, Phys. Rev. **116**, 778 (1959).

[14] A. Friedman, Rev. Mod. Phys. **37**, 201 (1965).

[15] H. F. Goenner, *General Relativity and Gravitation*, edited by A. Held (New York: Plenum, 1980).

[16] J. Rosen, Rev. Mod. Phys. **37**, 204 (1965).

[17] H. Narnhofer, I. Peter, and W. Thirring, Int. J. Mod. Phys. B **10**, 1507 (1996).

[18] A. Chamblin and G. W. Gibbons, Phys. Rev. D **55**, 2177 (1997).

[19] S. T. Hong, Y. W. Kim and Y. J. Park, Phys. Rev. D **62**, 024024 (2000).

[20] S. T. Hong, W. T. Kim, Y. W. Kim and Y. J. Park, Phys. Rev. D **62**, 064021 (2000).

[21] S. T. Hong, W. T. Kim, J. J. Oh and Y. J. Park, Phys. Rev. D **63**, 127502 (2001).

[22] S. T. Hong, Gen. Rel. Grav. **36**, 1919 (2004).

[23] H. Z. Chen, Y. Tian, Y. H. Gao and X. C. Song, JHEP **0410**, 011 (2004).

[24] N. L. Santos, O. J. C. Dias and J. P. S. Lemos, Phys. Rev. D **70**, 124033 (2004).

[25] Y. Tian, JHEP **0506**, 045 (2005).

[26] E. Radu, Int. J. Mod. Phys. A **21**, 4355 (2006).

[27] P. Langlois, Annals Phys. **321**, 2027 (2006).

[28] J. G. Russo and P. K. Townsend, Class. Quant. Grav. **25**, 175017 (2008).

[29] E. J. Brynjolfsson and L. Thorlacius, JHEP **0809**, 066 (2008).

[30] E. Greenwood and D. Stojkovic, JHEP **0909**, 058 (2009).

[31] B. Carter, *Black Holes*, edited by C. M. DeWitt and B. S. DeWitt (Gordon and Breach, New York, 1973).

[32] S. W. Hawking and D. N. Page, Commun. Math. Phys. **87**, 577 (1983).

[33] C. S. Peca and J. P. S. Lemos, Phys. Rev. D **59**, 124007 (1999).

[34] P. Mitra, Phys. Lett. B **459**, 119 (1999).

[35] S. W. Hawking and H. S. Reall, Phys. Rev. D **61**, 021014 (1999).

[36] B. Wang, E. Abdalla, and R.-K. Su, Phys. Rev. D **62**, 047501 (2000).

[37] S. T. Hong, J. Choi and Y. J. Park, Nonlinear Anal.-Theory Methods Appl. **63**, e493 (2005) [arXiv:math-ph/0407077].

[38] Y. S. Myung, Mod. Phys. Lett. A **23**, 667 (2008).

[39] Y. S. Myung, Y. W. Kim and Y. J. Park, Eur. Phys. J. C **58**, 337 (2008).

[40] Y. S. Myung, Y. W. Kim and Y. J. Park, Phys. Rev. D **78**, 084002 (2008).

[41] Y. S. Myung, Y. W. Kim and Y. J. Park, Phys. Lett. B **663**, 342 (2008).

[42] E. Witten, Adv. Theor. Math. Phys. **2**, 505 (1998).

[43] F. Belgiorno and S. L. Cacciatori, Class. Quant. Grav. **25**, 105013 (2008).

[44] A. Chamblin, R. Emparan, C. V. Johnson and R. C. Myers, Phys. Rev. D **60**, 064018 (1999).

[45] T. Tranah and P. T. Landsberg, Collective Phenomena **3**, 81 (1980).

[46] S. Hemming and L. Thorlacius, JHEP **0711**, 086 (2007).

[47] J. Nash, Ann. of Math. **60**, 383 (1954).

[48] J. Nash, Ann. of Math. **63**, 20 (1956).

[49] C. J. S. Clake, Proc. Roy. Soc. London Ser. A **314**, 417 (1970).